Investigation on the phosphorous interstitials in phosphorus implanted copper indium disulfide by a simplified total energy calculation

Y. J. Hsu and H. L. Hwang

Citation: J. Appl. Phys. **66**, 1651 (1989); doi: 10.1063/1.344379

View online: http://dx.doi.org/10.1063/1.344379

View Table of Contents: http://jap.aip.org/resource/1/JAPIAU/v66/i4

Published by the American Institute of Physics.

Investigation on the phosphorus interstitials in phosphorus-implanted copper indium disulfide by a simplified total energy calculation

Y. J. Hsu and H. L. Hwang
Department of Electrical Engineering, National Tsing Hua University, Hsinchu, Taiwan 30043, Republic of China

(Received 31 March 1989; accepted for publication 25 April 1989)

This paper presents a simplified total energy calculation for the phosphorus interstitials in P^+-implanted $CuInS_2$. The calculation was based on the tight-binding approximation and the atomic structure calculation scheme. Two types of interstitials were considered. One involved P and S^{2-}, the other involved P^{3+} and S^{3-}. Results showed that the latter would be more possible than the former, which confirms the results of our previous electron paramagnetic resonance study on the *p*-type doping of P^+-implanted $CuInS_2$.

I. INTRODUCTION

$CuInS_2$ is one of the ternary chalcopyrite compounds which have the potential of being future optoelectronic materials. A number of investigations on its preparation and characterization have been reported.[1–6] Our interest in $CuInS_2$ is derived from its potential as a photovoltaic material[7] and thus the formation of *p-n* junctions is essential to the device fabrication.

The conduction type of $CuInS_2$ can be controlled by annealing under different sulfur pressures.[8] Mittleman and Singh[9] reported on the conductivity of Cd and Zn doping in $CuInS_2$ and confirmed their shallow donor characteristics which were verified by Hwang *et al.*[10] The *p*-type conductivity control of $CuInS_2$ by introducing extrinsic impurities during the crystal growth (or by diffusion) is not feasible due to both the strong compensation effects and the low solid solubility of usual dopant species. Ion implantation can solve the solubility problem but the subsequent annealing is crucial in determining the final electrical activity because a large amount of defects are left in the near-surface region of the implanted crystal. In our previous work,[10,11] P^+ implantation was performed and the effects of both the subsequent thermal annealing and pulse electron beam (PEB) annealing on the electrical property were studied. In the case of thermal annealing, no rectified junction could be made from the normally grown and Zn-doped crystals, the electrical activity was even reduced by the thermal annealing, and large amounts of P_4S_5 precipitates in the annealed samples were found by transmission electron microscopy.[10] In the case of PEB annealing, a hole concentration as high as 9×10^{19} cm^{-3} was achieved and an excellent *p-n* junction with an ideality factor of 1.75 was obtained.[11]

In our previous work,[12] electron paramagnetic resonance (EPR) experiments were done on the P^+-implanted $CuInS_2$ samples to give physical insights into the two post-annealing processes. A model explaining the annealing effects was also established. In this work, a simplified total energy calculation is performed to further support the identification of the EPR signals and our model.

II. BRIEF DESCRIPTION OF THE EPR RESULTS

The details of the experimental procedures were described in Ref. 12. The results are summarized as follows: In addition to the signals of transition-metal contaminants, a narrow and single-line EPR signal with a *g* value of 2.0011 showed up in the as-implanted crystals. It was caused by the implantation and was attributed to the 4*s* orbitals of the sulfur atoms nearest to the phosphorus interstitials by considering the signal features, the electronegativity, and that most dopants locate at the interstitials in the implanted region.[13] This signal remained in the thermally annealed crystals but disappeared in the PEB-annealed samples. Thus the elimination of the phosphorus interstitials is the determinant factor to obtain good doping efficiencies. Defect elimination by the melting surface technique of PEB makes PEB annealing superior to thermal annealing.

III. THEORETICAL ANALYSIS

When the phosphorus implantation is done, most of the implants in $CuInS_2$ stop at the interstitial positions, each of which is surrounded by four sulfurs. After the relaxation process, if the phosphorus 3*p* electrons were not transferred to somewhere else, then, because of these electrons and because all the phosphorus nuclei have nonzero nuclear spins ($I=\frac{1}{2}$), multiline fine structures and hyperfine structures should be present in the EPR spectra. In our EPR measurement of the P^+-implanted $CuInS_2$, it seems peculiar at first glance that the sulfur 4*s* orbitals rather than the phosphorus 3*p* orbitals were detected. However, since neither the hyperfine structures nor the fine structures were observed, the spectra clearly excluded possibilities other than the electrons near the sulfur atoms. Besides, the electronegativity of sulfur atoms is larger than that of phosphorus atoms, which indicates that the electrons should be attracted from the surrounding atoms including copper, indium, and phosphorus atoms to sulfurs during the relaxation process. Our identification of the EPR signals could be further supported by the following simplified total energy calculation which compares the two cases: whether the phosphorus 3*p* electrons are attracted by sulfurs or not.

A. Calculation method

The system taken into consideration is the cluster formed by four sulfurs, their neighbors, and a phosphorus atom locating at the center (Fig. 1). By the ionic nature of

 0021-8979/89/161651-03$02.40

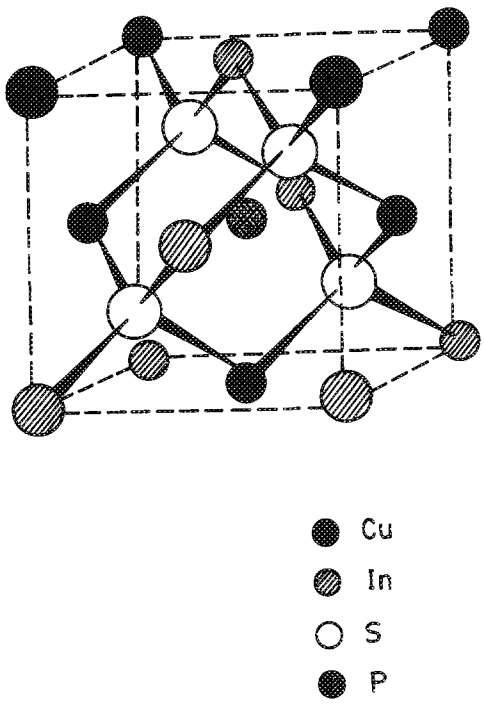

FIG. 1. The cluster of the phosphorus interstitial in $CuInS_2$ single crystal.

$CuInS_2$, it is reasonable to represent the various atoms and ions by the tight-binding approximation so that their overlaps can be neglected. This approximation is justified since even in the free-atom case the amplitudes of the atomic-orbital functions quickly drop to zero within a few angstroms as they go radially outward. Thus the whole system is composed of many small nonoverlapping systems (atoms or ions) which interact with one another through the Coulomb interactions between their respective effective charges, and the total energy E of the whole system can be approximated by the sum of the total energies E_a of these small systems and their Coulomb interaction energies U_{ab}. That is,

$$E_{\text{cluster}} = \sum_a E_a + \sum_{ab} U_{ab}, \tag{1}$$

where the first summation is over all the small systems and the second is over all the pairs of small systems which have nonzero effective charges. Therefore, the atomic structure calculations can be applied.

In our calculation, two charge configurations were considered: one was with P and S^{2-}, the other was with P^{3+} and S^{3-}. In both cases Cu^+ and In^{3+} were kept unaltered. The total energy of the whole cluster was calculated for these two cases and their difference was used to clarify the validity of the EPR signals.

The procedure of the calculation for the structures of atoms and ions is similar to the conventional Herman–Skillman-type atomic structure calculation scheme.[14–16] The solved equation is the central-field atomic one-particle equation

$$\left(\frac{d^2}{dr^2} - \frac{l(l+1)}{r^2} + [E_{nl} - V(r)]\right) P_{nl}(r) = 0, \tag{2}$$

with n and l being the orbital quantum numbers, E_{nl} being the orbital eigenenergy, $P_{nl}(r)/r = R_{nl}(r)$ where $R_{nl}(r)$ is the radial part of the orbital, and $V(r)$ including the Coulomb potential due to the electrons and the nucleus as well as the local density exchange and correlation functionals.[17–19]

With initial eigenenergies (E_{nl}) and an initial potential [$V_i(r)$] specified, the outward and inward integrations of Eq. (2) are performed for each orbital. The eigenenergies are improved until good matching between the two integrations is achieved. The generated orbitals are then used to compute a new potential [$V_f(r)$] and if the self-consistency of $V(r)$ is not attained, the next iteration is started with a new potential and new eigenenergies. The new potential is a suitable combination of $V_i(r)$ and $V_f(r)$ to avoid unstability. The new eigenenergies are obtained by using the first-order perturbation method. The matching criterion was chosen to be that the absolute value of $\Delta E_{nl}/E_{nl}$ is less than 10^{-5}. And the self-consistency criterion was set to be $|V_i(r) - V_f(r)|_{\max} < 10^{-3}$. Actually, we found that $|\Delta E_{nl}/E_{nl}|$ smaller than 10^{-10} was easily attainable and about 5–10 iterations were needed to satisfy the self-consistency when the Thomas–Fermi potential and the corresponding eigenvalues computed by Latter[20] were used as the starting quantities.

When dealing with negative ions, the difficulty in binding electrons to make the orbitals damped was overcome by a suitable tail correction to the potential which takes into account the screening effect. The basic idea of this tail correction is the same as the conventional one[16,20] which deals with neutral atoms and positive ions, but the radial probability rather than the potential is used as the checking variable. In this correction, the radial probabilities of each occupied orbital are integrated and summed to find the radii at which the neutral and the various negative effective charge states emerge and then suitable Coulomb potentials are specified in the regions between these radii.

Since the atomic orbitals are less extended in solids than in free atoms, the infinity of the radial integration domain of Eq. (2) was chosen in our calculation to be nearer than in the free-atom case. This arrangement not only simulates the compression behavior of the atomic orbitals in solids but also assures the nonoverlapping of the atoms and the ions.

B. Results and discussion

The total energy of the cluster with the first charge configuration is calculated to be higher than that of the second by an amount of 0.922 Ry. Thus the second configuration is more energetically stable than the first and our interpretation of the EPR signal is confirmed. Since this configuration is thermally stable, it is not easily eliminated by the thermal annealing steps and the EPR signal associated with this defect should appear both in the as-implanted and the thermally annealed samples as expected. The identification of P_4S_5 precipitates[10] also agreed with our result. On the other hand, PEB annealing melts the samples to a certain depth and then the recrystallization happens, thus the phosphorus interstitials can be easily eliminated and the phosphorus atoms have a chance to occupy the sulfur lattice sites during the recrystallization process. Therefore, the EPR signal could not be

detected in the PEB annealed samples and better doping efficiencies were obtained.

Since the quantity of interest is the difference between the total energies and the magnitude of the exchange and correlation energy is very small compared with that of the Coulomb energy, the choice of the formalism for the exchange and correlation term is not so important in our calculation. It was also noted that the total energy of S^{2-} differs little from that of S^{3-} but the total energy of P is less than that of P^{3+} by about 20 Ry, and it is the Coulomb interaction energy that makes the latter configuration stable. The tight-binding property is essential in defining the effective charges of the small system in the cluster.

The validity of our approximation should be further examined by a more general calculation. However, this work gives us a first theoretical confirmation about our experimental results.

IV. CONCLUSION

The identification of the EPR signals in P^+-implanted $CuInS_2$ crystals has been theoretically confirmed by a simplified total energy calculation. The key role of the melting effect during the PEB annealing on the resultant electrical property is further clarified.

ACKNOWLEDGMENT

The authors wish to acknowledge the financial support from the National Science Council of the Republic of China.

[1]H. Hahn, G. Frank, W. Klinger, A. D. Meyer, and G. Storger, Z. Anorg. Allg. Chem. **271**, 153 (1953).
[2]B. Tell, J. L. Shay, and H. M. Kasper, Phys. Rev. B **4**, 2463 (1971).
[3]D. C. Look and J. C. Manthmuthil, J. Phys. Chem. Solids **37**, 173 (1976).
[4]J. L. Shay and J. H. Wernick, *Ternary Chalcopyrite Semiconductors: Growth, Electronic Properties, and Applications* (Pergamon, New York, 1976).
[5]H. Neumann, W. Horig, V. Savelev, J. Lagzdonis, B. Schumann, and G. Kuhn, Thin Solid Films **79**, 167 (1981).
[6]H. L. Hwang, M. H. Yang, C. Y. Sun, and T. M. Hsu, Proc. Nat. Sci. Counc. ROC(A) **10**, 72 (1986).
[7]J. M. Meese, J. C. Manthurtuthil, and D. R. Locker, Bull. Am. Phys. Soc. **20**, 696 (1975).
[8]B. Tell, J. L. Shay, and H. M. Kasper, J. Appl. Phys. **43**, 2469 (1972).
[9]S. D. Mittleman and R. Singh, Solid State Commun. **22**, 659 (1977).
[10]J. L. Lin, L. M. Liu, J. T. Lue, M. H. Yang, and H. L. Hwang, J. Appl. Phys. **59**, 378 (1986).
[11]J. L. Lin, J. T. Lue, M. H. Yang, and H. L. Hwang, Appl. Phys. Lett. **48**, 1957 (1986).
[12]Y. J. Hsu and H. L. Hwang (to be published).
[13]Y. J. Hsu, H. L. Hwang, and C. Y. Sun, J. Cryst. Growth **86**, 749 (1988).
[14]D. R. Hartree, in *The Calculation of Atomic Structures* (Wiley, New York, 1957).
[15]F. Herman and S. Skillman, in *Atomic Structure Calculations* (Prentice-Hall, Englewood Cliffs, NJ, 1963).
[16]D. A. Liberman, D. T. Dromer, and J. T. Waber, Comput. Phys. Commun. **2**, 107 (1971).
[17]P. Hohenberg and W. Kohn, Phys. Rev. B **136**, 864 (1964).
[18]W. Kohn and L. J. Sham, Phys. Rev. A **140**, 1133 (1965).
[19]L. Hedin and B. I. Lundqvist, J. Phys. C **4**, 2064 (1971).
[20]R. Latter, Phys. Rev. **99**, 510 (1955).